Dynamics of the Junction Point in Model Network Polymers by ^{31}P Nuclear Magnetic Relaxation

Jie-Feng Shi, L. Charles Dickinson, William J. MacKnight,* and James C. W. Chien*

Department of Polymer Science and Engineering and Department of Chemistry, University of Massachusetts, Amherst, Massachusetts 01003

Received April 9, 1993; Revised Manuscript Received May 17, 1993®

ABSTRACT: Solid-state ^{31}P NMR spin–lattice relaxation times (T_1^P) have been measured over a wide range of temperatures for a series of network polymers with molecular weights between cross-links (M_c) ranging from 250 to 2900. The networks were formed from poly(tetrahydrofuran) and tris(4-isocyanatophenyl) thiophosphate. The chain length dependence of the glass transition temperature obeys the Fox–Loshaek relation. The dominant mechanism for ^{31}P spin–lattice relaxation was found to be chemical shift anisotropy. The data fitted equally well to the Cole–Cole or the Williams–Watts relaxation functions. The apparent and microscopic activation energies for the motion of junction points are 44–73 and 23–30 kJ/mol, respectively, for different M_c samples. The degree of motional correlation can be described quantitatively by the coupling parameters. The effect of increasing M_c is to reduce the width of the distributions and the cooperative motional mode in the cross-link point.

Introduction

Network polymers exhibit a broad range of valuable properties for many applications. Correlations between the structure of a network polymer, the frequency distribution of the motions, and its macroscopic physical properties continue to be the focus on research on elastomers. The challenge is to find quantitative relationships. Solid-state NMR is uniquely suited for this task. For instance, the dynamics of the phosphorus-centered junction point in model network polymers derived from poly(propylene glycol) (PPG) and tris(4-isocyanatophenyl) thiophosphate (TIPTP) can be monitored precisely by ^{31}P NMR relaxation, while those of the chain segments may be independently observed by ^{13}C NMR.[1-5] The low-frequency motion of the junction point in this network was observed with ^{31}P solid-state 2D-exchange NMR[5] and directly correlated with the mechanical properties. The central purpose of this work is to extend the solid-state NMR investigation to another model network system derived from monodisperse poly(tetrahydrofuran) (PTHF) with TIPTP. The focus here is to understand the role of the junction point in molecular dynamics by detailed analysis of NMR spin–lattice relaxations of the ^{31}P nuclei as a function of temperature and molecular weight between cross-links (M_c). We succeeded in previous work in obtaining a quantitative correlation of mechanical relaxation properties with dielectric and nuclear magnetic relaxation data.[5]

Experimental Section

Model network polymers were prepared from monodisperse α,ω-dihydroxy-PTHF (Aldrich) of MW = 250, 650, 1000, 2000, and 2900, and TIPTP (Mobay) by a previously described procedure.[1] The samples are designated N250, N650, N1000, N2000, and N2900, respectively. One N650 sample was swollen by the telechelic PTHF with MW = 250 up to 3 days, and this sample is referred to as "swollen".

DSC measurements were made on a Du Pont 2000 thermoanalysis system. The heating rate was 10 °C/min. The glass transition temperature was defined as the midpoint of the heat capacity change from the curves recorded. The measurements were taken after one heating/cooling cycle.

The ^{31}P NMR measurements were carried out with an IBM AF200 spectrometer with a solids accessory at a frequency of 81 MHz. The network samples were ground to a powder in order to be spun at 5 kHz. Both the ^{31}P and the ^{1}H $\pi/2$ pulses were 5 μs, and the recycle times varied from 5 to 70 s depending upon the sample and measurement. The ^{31}P static powder spectra were obtained by using a spin–echo pulse sequence with or without ^{1}H decoupling. The ^{31}P spin–lattice relaxation times (T_1^P) were measured by two parallel methods, cross-polarization (CP) and direct polarization (DP). The contact time was 1.5 ms for CP/MAS measurements. Temperature was controlled by a Bruker temperature control unit with an accuracy of ±1 °C.

Computer simulation to estimate the ^{31}P–^{1}H distance was performed on a Macintosh computer using an MM2 force field program.

The T_1^P fitting procedure was performed on the University of Massachusetts VAX Cluster. Computer programs based on a downhill simplex method were used to minimize the sum of the squares of the residuals.

Results

Glass Transition and Crystallinity in Networks. DSC results are summarized in Table I. DSC showed that N2000 and N2900 are crystalline networks having melting points at 290 and 286 K with crystallinities of 15 and 27%, respectively. All the other network polymers are amorphous materials.

The T_g decreases with M_c. Several equations are available to interpret such data. The simple Fox–Loshaek relationship, based on free volume theory,[6]

$$T_g = T_g^\infty + C/M_c \quad (1)$$

is used to fit the experimental data (Figure 1). The fit was good for all the specimens with the exception of N250. The datum of this sample deviates from eq 1 because the material is not elastomeric due to its very high cross-linking density. The values of T_g^∞ and C were found as 188 K and 4.3×10^4 by linear regression analysis. The T_g for linear high molecular weight PTHF is 189 K, in agreement with the T_g^∞ calculated for the network polymers.

CSA Relaxation Mechanism. The dominant nuclear spin relaxation mechanism in solids is usually either dipole–dipole (DD) (for $I = 1/2$ nuclei) or quadrupolar (for $I > 1/2$ nuclei) interaction. The latter is inapplicable to the $I = 1/2$ ^{31}P nuclei. Furthermore, the distance between

® Abstract published in *Advance ACS Abstracts*, September 15, 1993.

0024-9297/93/2226-5908$04.00/0

Table I. Glass Transition Temperature and Crystallinity in PTHF Networks by DSC

sample	T_g (K)	T_m (K)	crystallinity (%)
N250	306	none	0
N650	254	none	0
N1000	231	none	0
N2000	209	290	15
N2900	203	286	27

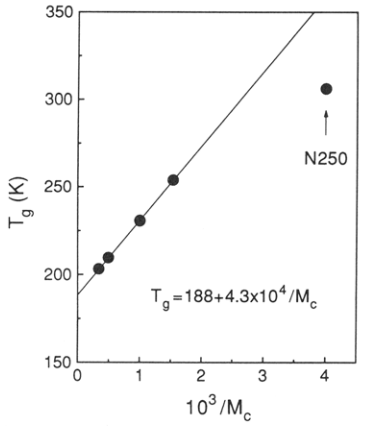

Figure 1. Dependence of T_g on M_c fitted by the Fox–Lashaek equation.

one ^{31}P atom and another ^{31}P is very large so the homonuclear dipole–dipole relaxation is very inefficient.

The nearest ^{31}P–^{1}H (aromatic proton) distance was estimated by computer simulation in Figure 2. The nearest distance varies from 2.9 to 4.2 Å as the aromatic ring rotates along its principal symmetry axis. This distance is too large for heteronuclear DD relaxation to be effective.

It is the chemical shift anisotropy (CSA) relaxation mechanism which is important for the ^{31}P relaxation in the present networks. The percentage of the relaxation rates (R_1) was roughly estimated by using[7,8]

$$R_1(\mathrm{CSA}) = T_1^{-1} = (1/15)\gamma_P^2 B_0^2 \Delta\sigma^2 [J(\omega_P)] \quad (2)$$

$$R_1(\mathrm{DD}) = T_1^{-1} = (1/20)\gamma_P^2\gamma_H^2 h^2 \sum r_i^{-6} [J(\omega_H - \omega_P) + 3J(\omega_P) + 6J(\omega_H + \omega_P)] \quad (3)$$

with the spectral density $J(\omega)$ given by the simple isotropic diffusion model.

$$J(\omega) = 2\tau_c/(1 + \omega^2\tau_c^2) \quad (4)$$

Here, γ_P and γ_H are the phosphorus and proton gyromagnetic ratios, respectively, ω_P and ω_H are the corresponding resonance frequencies, B_0 is the magnetic field intensity, $\Delta\sigma$ is the chemical shift anisotropy, r_i is the distance between the phosphorus and the ith proton, and τ_c is the correlation time. In the limiting cases, the DD contribution is ca. 15% for the three protons 2.8 Å away from P, while it is nearly 0% for the proton 4.2 Å from P. The average DD contribution varies with the rotation of the aromatic ring. The DD interactions of ^{31}P with ^{31}P or ^{31}P with aliphatic proton are unimportant because of the large bulk of the cross-link moiety.

The static spin–echo line shape of the N250 was observed without high-power proton decoupling. The ^{31}P spectrum in Figure 3 shows a simple CSA powder pattern of an axially symmetric top. For DD interaction, it would have been bell shaped. The application of proton decoupling did not alter the line shape, consistent with the unimportance of the heteronuclear DD mechanism. The ^{31}P line shape and ^{31}P relaxation times, previously obtained on the PPG–TIPTP network,[3] were also dominated by the CSA interaction.

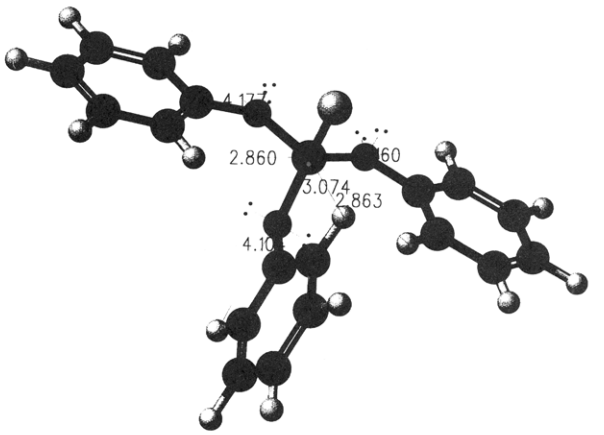

Figure 2. Computer simulation of the cross-linker group in a model PTHF network.

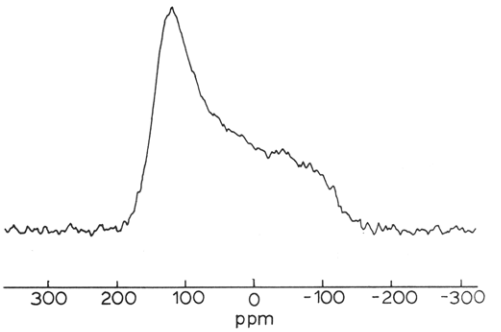

Figure 3. Line shape of the ^{31}P NMR spectrum without ^{1}H decoupling for the N250 network.

The anisotropy factors $\Delta\sigma$ ($=\sigma_\perp - \sigma_\parallel$) were determined from spin–echo line shapes with proton decoupling below the T_g. Fitting the theoretical CSA tensor to the line shapes gives $\Delta\sigma = 281 \pm 3$ ppm for all samples.

^{13}P Spin–Lattice Relaxation Time. The motion of the junction point in our network polymer was investigated by ^{31}P spin–lattice relaxation times. Two parallel methods for T_1 measurement were used. One is cross-polarization (CP), which preferentially samples the rigid region; the other is direct polarization (DP), which detects all the regions if recycle times are sufficiently long. The ^{31}P T_1 values by CP or DP show a single relaxation decay at the temperature we measured, with nearly the same values of T_1 (Table II). This agreement suggests a uniform distribution of cross-linking points in the network.

The log T_1 vs $1/T$ curves change with M_c (Figure 4). With increasing M_c, the T_1 minimum monotonically decreases and the temperatures of the T_1 minimum moves to lower temperature. This is consistent with the increased mobility of the junction point with increasing chain length. The stochastic process can be described by an autocorrelation function $G(\tau)$ and spectral density $J(\omega)$, which is the Fourier transform of $G(\tau)$.

$$G(\tau) = \langle F(0)\, F^*(\tau) \rangle \quad (5)$$

$$J(\omega) = \int_{-\infty}^{\infty} G(\tau) \exp(-i\omega\tau)\, d\tau \quad (6)$$

$G(\tau)$ is given as an exponential function from Debye's model for random motion, referred to as BPP:

$$G(\tau) = \exp(-|\tau|/\tau_c) \quad (7)$$

Table II. ^{31}P T_1 Relaxation Times (s) of PTHF Networks

	PTHF250		PTHF650			PTHF1000		PTHF2000		PTHF2900	
temp (K)	CP	DP	CP	DP	swollen DP	CP	DP	CP	DP	CP	DP
268										3.08	
278								2.36		2.11	
288								1.67		1.45	1.51
298	10.07	11.01	2.95	3.26	1.86	1.98	1.84	1.16	1.29	1.01	1.03
308	7.04	8.07	2.27	2.38	1.38	1.52	1.51	1.00	1.01	0.80	0.81
318	5.18	5.17	1.61	1.66	1.06	1.21	1.15	0.87	0.85	0.71	0.74
328	3.61	4.25	1.27	1.41	0.93	1.01	0.94	0.74	0.77	0.71	0.71
338	2.96	2.99	1.04	1.13	0.80	0.90	0.84	0.75	0.74	0.73	0.71
348	1.99	2.48	0.93	1.02	0.72	0.82	0.80	0.74	0.77	0.80	0.77
358	1.50	1.78	0.86	0.90	0.70	0.81	0.79	0.79	0.77	0.84	0.80
368		1.42	0.84	0.87	0.79	0.80	0.82	0.84	0.90	0.85	0.87
378		1.25	0.84	0.85	0.82	0.85	0.88	0.94	0.93	0.92	0.89

$$J(\omega) = 2\tau_c/(1 + \omega^2\tau_c^2) \quad (8)$$

The rate of spin-lattice relaxation, R_1, for axially symmetric CSA can be expressed as follows:

$$R_1 = T_1^{-1} = (1/15)\gamma_I^2 B_0^2 \Delta\sigma^2 [J(\omega_I)] \quad (9)$$

Since T_1 corresponds to very high frequency motion (30 ps $< \tau_c <$ 1 μs), we may taken an Arrhenius form for the temperature dependence.

$$\tau_c = \tau_0 \exp(E_A/RT) \quad (10)$$

where E_A is the activation energy and T is the absolute temperature in kelvin. Figure 4 shows clearly that the motion of the junction point is not isotropic and random. The theoretical value of the T_1 minimum according to BPP is lower than the experimental value of the T_1 minimum by about a factor of 2. The same discrepancy was found in the PPG–TIPTP network.[3] The motion of junction points in our system is not isotropic motion, either because the motion of the three chains attached to each junction point are correlated or the motional barrier heights are different for each junction point site.

Distribution of Correlation Times. In solid polymers, motion is often a complex nonrandom process. This can be treated by introducing the concept of a distribution of exponential correlation times.[9-11]

$$G(\tau) = \int_0^\infty \rho(\tau_c) \exp(-|\tau|/\tau_c)\, d\tau_c \quad (11)$$

with a normalization condition for the distribution function $\rho(\tau_c)$

$$\int_0^\infty \rho(\tau_c)\, d\tau_c = 1 \quad (12)$$

Then the spectral density becomes

$$J(\omega) = \int_0^\infty \rho(\tau_c)[2\tau_c/(1 + \omega^2\tau_c^2)]\, d\tau_c \quad (13)$$

It was recognized early that a distribution of correlation times can raise the NMR T_1 minimum.[9] The physical interpretation of such distributions has become a complex matter. A common dichotomy is between homogeneous and heterogeneous distributions, with the distinction hinging on whether there is a variety of motional processes with the same or different coupling models which include correlated or cooperative motion and thus lead to "dynamic heterogeneities". It is not simple to differentiate these cases experimentally, and the coexistence of a variety of distributions has been demonstrated in polymers.[11-13]

Many of the spectral densities used in NMR originate from the interpretation of dielectric relaxation experiments. The Havriliak–Negami (HN) and Williams–Watts (WW) functions have been successfully applied to interpret dielectric relaxation and 2D-exchange NMR data for the PPG–TIPTP model network. Shioya et al.[14] showed that the HN and WW functions have similar behavior. Both of them can fit the same data set of dielectric relaxation satisfactorily in some cases.

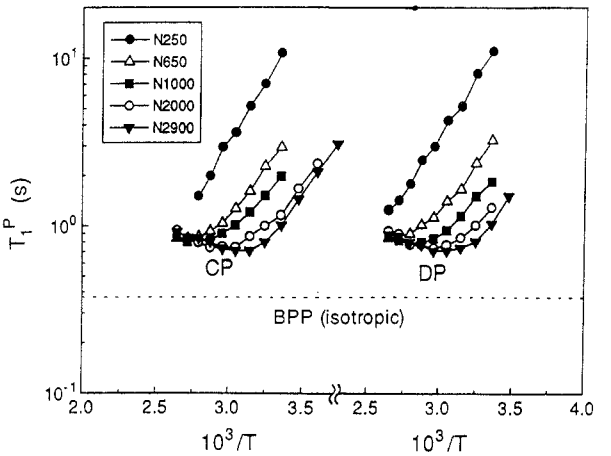

Figure 4. Temperature dependence of ^{31}P T_1 by the CP (left) and by the DP (right) for a series of PTHF networks. The dashed line corresponds to the T_1 minimum of BPP model.

The HN spectral density in dielectric relaxation is[15]

$$H(\omega) = 1/[1 + (i\omega\tau)^{1-\alpha}]^\beta \quad (14)$$

where β is the parameter for an asymmetric distribution and α is the parameter for a symmetric distribution. The HN spectral density is reduced to the Cole–Cole spectral density if $\beta = 1$ and to the Davidson–Cole spectral density if $\alpha = 0$.[11,16] Ichikawa and MacKnight[4] used the sum of two HN functions to describe the dielectric relaxation for the PPG network. They considered the higher frequency process to be due to motions involving the ether oxygen group in the chain and the lower frequency process to be associated with the motions involving the urethane group of the cross-linker.[4] The parameter β is almost constant for both processes, but α varies from 0.193 to 0.561.

To obtain more stable fitting results, we choose the Cole–Cole (CC) spectral density with one fitting parameter. The change in the parameter β is rather small for motions of different groups, and the distribution of correlation times is symmetrical.

The CC spectral density function for NMR relaxation is given by[11]

$$J(\omega) = (2/\omega)\sin[(1-\alpha)\pi/2]\{(\omega\tau_c)^{1-\alpha}/[1 + (\omega\tau_c)^{2(1-\alpha)} + 2\cos[(1-\alpha)\pi/2](\omega\tau_c)^{1-\alpha}]\} \quad (15)$$

The parameter α has a value between 0 and 1 and depends on the details of the averaging process, $\alpha = 0$ implies unique activation energies and no correlated motion, while $\alpha =$ 1 implies the maximum distribution of activation energies with a considerable degree of correlated motion.

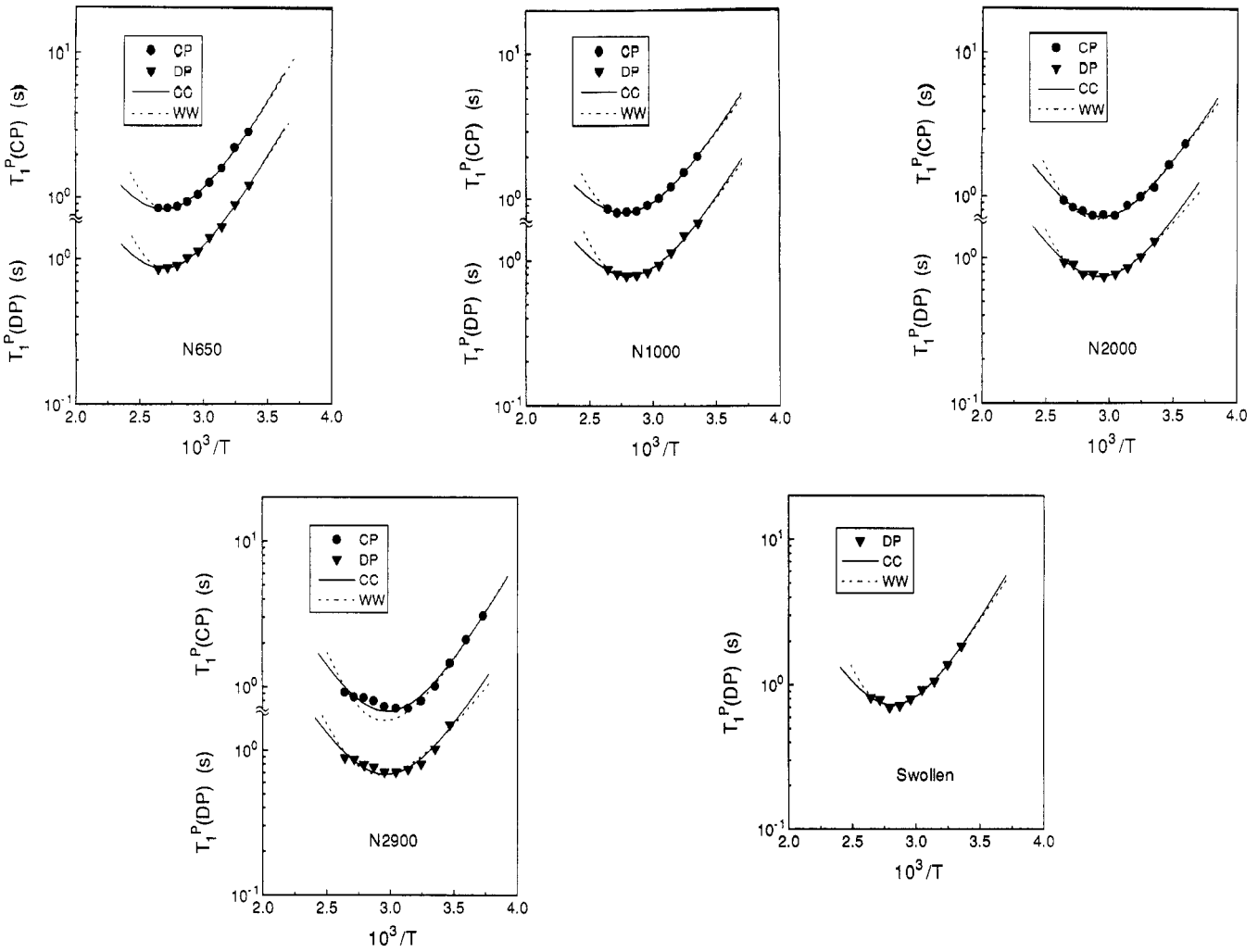

Figure 5. ^{31}P T_1 of PTHF network vs inverse temperature. The solid and the dashed lines correspond to best fits calculated from the Cole–Cole and the Williams–Watts distributions of correlation times, respectively.

In practice, one writes the correlation times in an Arrhenius form:

$$\tau_c = \tau_\infty^* \exp(E_A^*/RT) \tag{16}$$

where τ_∞^* and E_A^* are the apparent preexponential factor and activation energy, respectively. The latter reflects the contribution to the barrier height from molecular interactions encountered in a polymeric material.[17] For the CC distribution, it is expressed by

$$E_A^* = E_A/(1-\alpha) \tag{17}$$

where the activation energy, E_A, corresponds to the barrier encountered in the isolated cross-linking point and is usually comparable to the barriers calculated for simple rotations.

We also used the empirical Williams–Watts correlation function to analyze our data. It had been used successfully to interpret NMR and dielectric relaxation data for many polymer systems. Ngai et al. have developed a coupling model and tried to derive the Williams–Watts function from it.[18,19] Recently, the WW distribution was employed to simulate the 2D-exchange NMR results and to relate them to mechanical and dielectric loss peaks for the PPG–TIPTP network.[5] The common form of the WW is

$$\phi(t) = \exp[-(t/\tau_p)^\alpha] \qquad 0 < \alpha < 1 \tag{18}$$

The parameter in the WW function is $\alpha = 1 - n$, where n is a parameter describing the coupling strength. A value of $n = 0$ corresponds to the isotropic motion, and a value of $n = 1$ corresponds to the broadest distribution. It is convenient to interpret a general correlation function in terms of a superposition of an exponential correlation function.[20–22]

$$\phi(t) = \int_0^\infty \rho(\tau) \exp(-t/\tau)\, d\tau \tag{19}$$

where $\rho(\tau)$ is a WW distribution function and can be approximated to a series expansion given by Bendler et al.[20]

To simplify the numerical calculation, we treated the continuous distribution as a discrete summation

$$\phi(t) = \sum P_j \exp(-t/\tau_j) \tag{20}$$

with a normalization condition of $\phi(0) = 1 = \sum P_j$. It has been reported that the exponent α will change linearly with absolute temperature.[14,20] We assumed that α is temperature independent and that a temperature shift only causes a uniform logarithmic shift of correlation times.[12,21] The relationship between the apparent activation energy and the microprocess activation energy for the WW distribution is given by[17]

$$E_A^* = E_A/(1-n) = E_A/\alpha \tag{21}$$

Comparison of the CC and WW Distributions. The ^{31}P nuclear relaxation times, T_1, with either CP or DP were fitted satisfactorily by both the CC and the WW distributions as shown in Figure 5. Deviation was seen in the high-temperature range for N2900. The ratio of the standard deviation of the two functions, $\sigma(WW)/\sigma(CC) = 1.29 \pm 0.24$, is not much greater than unity. From a

Table III. Fitting Parameters Used for ^{31}P T_1 Relaxation Times

sample	E_A^* (kJ/mol) CC	E_A^* (kJ/mol) WW	E_A (kJ/mol) CC	E_A (kJ/mol) WW	τ_∞^* (s) CC	τ_∞^* (s) WW	α CC	n WW	SD σ^a CC	SD σ^a WW	σ(WW)/σ(CC)
N250 (CP)[b]			27.22		1.8×10^{-12}				0.173		
N250 (DP)[b]			26.84		2.3×10^{-12}				0.256		
N650 (CP)	54.1	68.9	29.3	27.6	5.1×10^{-17}	2.3×10^{-19}	0.46	0.59	0.0733	0.0688	0.938
N650 (DP)	57.5	72.9	29.9	28.7	1.7×10^{-17}	6.5×10^{-20}	0.48	0.61	0.0649	0.0707	1.09
swollen (DP)	49.2	56.4	29.5	27.3	1.1×10^{-16}	7.3×10^{-18}	0.40	0.52	0.0365	0.0385	1.06
N1000 (DP)	48.8	58.5	27.1	25.1	1.7×10^{-16}	4.5×10^{-18}	0.45	0.57	0.0114	0.0155	1.36
N1000 (CP)	49.7	58.7	27.8	25.5	1.0×10^{-16}	3.5×10^{-18}	0.44	0.57	0.0565	0.0499	0.882
N2000 (CP)	45.5	50.0	27.7	25.2	2.0×10^{-16}	3.6×10^{-17}	0.39	0.50	0.0445	0.0697	1.57
N2000 (DP)	46.1	49.6	27.4	23.1	1.7×10^{-16}	4.3×10^{-17}	0.40	0.53	0.0353	0.0552	1.56
N2900 (CP)	44.1	44.4	28.4	28.3	2.6×10^{-16}	1.9×10^{-16}	0.36	0.37	0.0795	0.141	1.78
N2900 (DP)	43.1	45.2	27.5	23.4	4.0×10^{-16}	1.7×10^{-16}	0.36	0.48	0.0807	0.110	1.36

[a] Standard deviations of fits were calculated according to ref 14. [b] N250 was fitted by BPP theory.

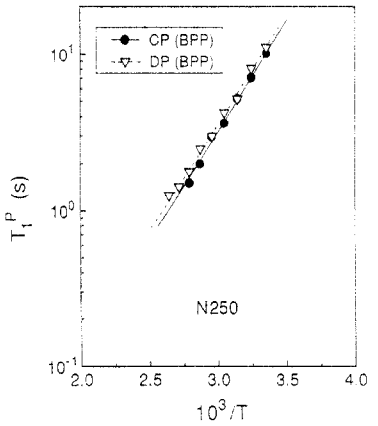

Figure 6. ^{31}P T_1 of N250 network vs. inverse temperature. The solid and dash lines correspond to best fits of CP and DP data calculated from the partial BPP model, respectively.

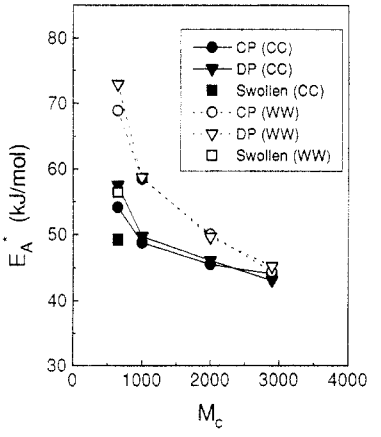

Figure 7. Plot of E_A^* fitted by the CC (●, ▼, ■), and the WW (○, ▽, □) distributions as a function of M_c.

statistical point of view the CC distribution seems to be slightly better than the WW distribution. The fitting parameters obtained from T_1 with CP or DP are close (Table III). This is not surprising since both T_1 with CP and DP detect the same region of cross-linking points. Both fitting procedures with the CC and WW distributions are quite stable. The T_1^P data of N250 were obtained for the low-temperature region. This sample was fitted using the BPP model instead of the distribution functions (Figure 6). The activation energy from fitting should correspond to the E_A.

Figure 7 shows that E_A^* decreases gradually with increasing chain length. It may be expected that E_A^* will become independent of M_c at high molecular weights. Upon further examination, we found a linear relationship between E_A^* and inverse M_c (Figure 8). By analogy with

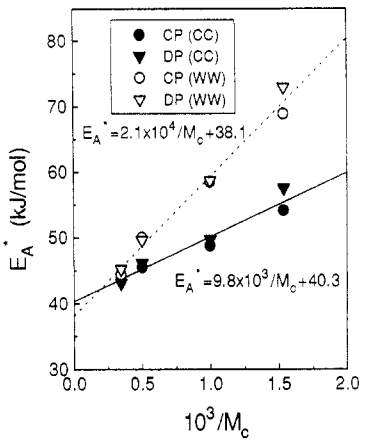

Figure 8. Linear relationship between E_A^* and inverse M_c: (●, ▼) fitted by the CC distribution; (○, ▽) fitted by the WW distribution.

the Fox–Loshaek equation, we have

$$E_A^* = E_A^\infty + C/M_c \tag{22}$$

where E_A^∞ corresponds to the motion of the junction point as M_c approaches infinity and C is a constant. E_A^∞ and C were obtained from linear regression as 40.3 kJ/mol and 9.8×10^5 for the CC distribution and as 38.1 kJ/mol and 2.1×10^4 for the WW distribution, respectively. The values of E_A^* are larger than Ichikawa and MacKnight's results for the lower frequency process associated with the urethane group.[4] It could be that the nuclear motion of the cross-linking point (by NMR) is more restricted than that of the bulk cross-linker group by DETA). Of course, the two experimental methods are different as are the two network systems.

The activation energies for microscopic processes, E_A, are almost constant (E_A = 27.1 ± 0.9 kJ/mol) for both distributions and T_1 with CP or DP of all the samples. This suggests that all the cross-linking points have very close intrinsic motional properties if isolated.

The width parameters, α for the CC distribution and n for the WW distribution, decrease monotonically with increasing M_c in network polymers (Figure 9). Thus the effect of increasing chain length is to reduce the width of the distribution and also to reduce the cooperative motion in the cross-linking point.

When N650 was swollen by linear PTHF with a molecular weight of 250, both the apparent activation energies and the width parameters describing the coupling strength decrease for the CC and WW distributions. Table III shows that the apparent activation energies drop from 57.5 to 49.2 kJ/mol for the CC distribution and 72.9 to 56.4 kJ/mol for the WW distribution. The width param-

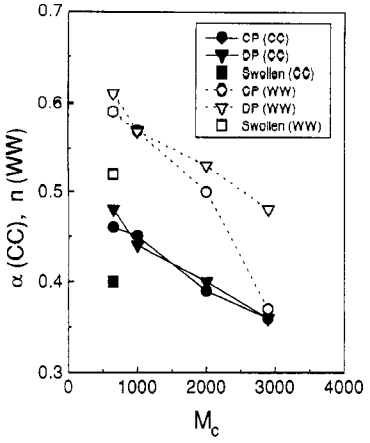

Figure 9. Plot of width parameters of the distributions as a function of M_c: (●, ▼) fitted by the CC distribution; (○, ▽) fitted by the WW distribution.

eter α drops from 0.48 to 0.40 for the CC distribution, and n drops from 0.61 to 0.52 for the WW distribution.

Discussion of Results

The BPP isotropic rotational diffusion model for polymer motion is usually found to be inadequate for detailed analysis of NMR relaxation data. Even random coil polymer chains can undergo many types of motion involving different mechanisms. The concept of an empirical distribution of exponential autocorrelation functions is a simple way to deal with this complex problem. A distribution of correlation times is formally equivalent to nonexponential decay of the autocorrelation function. The usage of distribution functions provides some insight into the interaction of polymer motions. The Havriliak and Williams–Watts functions have been compared by Shioya et al.[14] They found both functions were capable of fitting the dielectric relaxation data of poly(vinyl acetate) over a wide temperature region.

The crystalline samples, N2000 and N2900, will undergo a melting transition (T_m) during the temperature scan in the T_1 measurement. However, there was no discontinuity observed by us in the T_1 variation with temperature. Axelson[23] also reported a smooth change of T_1 when traversing T_m. This may be characteristic of linear polymeric materials having a broad melting transition with a low enthalpy of fusion. For the present system the cross-linking point is outside of the crystal domain, and its motion will lag behind T_m depending upon the coupling between them. Also the T_1 curves become broader when the temperature increases, indicating a decrease of activation energy. It is difficult to quantify, by T_1 measurement alone, the relationship of the temperature dependence of the activation energy during the melting transition. E_A* for N2000 and N2900 obtained from fitting represents the average value for the temperature range measurement. The calculated log T_1 vs $1/T$ curves from the most asymmetric distributions display the deeper curve on the high-temperature side and are flatter on the low-temperature side. This behavior contradicts the T_1 data of N2000 and N2900 due to the melting transition. Thus the symmetric CC distribution fitted the data slightly better than the asymmetric WW distribution.

The apparent preexponential factor τ_∞* fitted with distribution function models usually does not have a definite physical meaning. It is not simply an Arrhenius prefactor but is rather a combination of several parameters.[17] The value of E_A* found by the WW distribution is greater than that determined by the CC distribution.

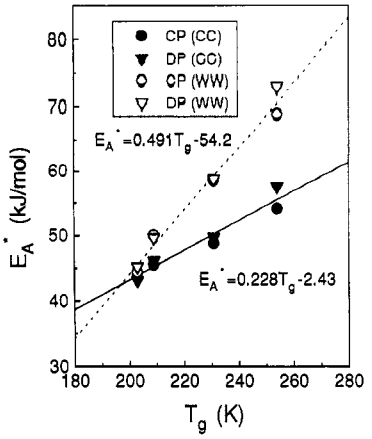

Figure 10. Linear relationship between E_A* fitted by NMR data and T_g measured by DSC: (●, ▼) fitted by the CC distribution; (○, ▽) fitted by the WW distribution.

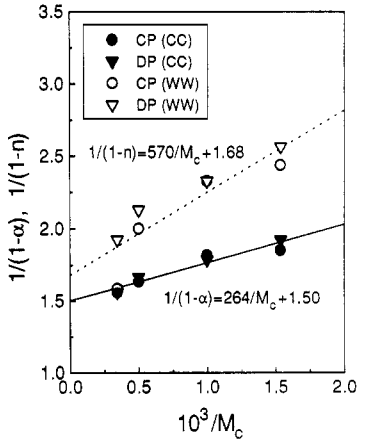

Figure 11. Linear relationship between inverse (1 − width parameter) and inverse M_c: (●, ▼) fitted by the CC distribution; (○, ▽) fitted by the WW distribution.

It seems that the CC distribution modifies the curve more strongly than the WW distribution does. In other words, to reach the same increase of T_1 minimum, the value of $(1 - n)$ for the WW distribution is smaller than that of $(1 - \alpha)$ for the CC distribution. The discrepancy between the two distributions is manifested in their different apparent activation energies. The E_A* and the breadth of distributions decrease monotonically with increasing M_c. This trend appears to be a general one for network polymers since an increase in M_c causes an increase of molecular mobility and reduces the long-range cooperative motions. The width parameters, α for the CC distribution and n for the WW distribution, quantitatively described the nature of the motion of the junction points in the network polymers. The two parameters change toward the direction of isotropic motion when M_c increases.

Figure 8 shows a linear relationship between the apparent activation energy fitted by NMR and inverse M_c. Since the DSC results showed that the M_c dependence of the glass transition temperature also obeys the Fox–Loshaek relation, the E_A* and T_g are expected to have a linear relationship (Figure 10). It is clear that the motion of cross-links seen in the NMR relaxation experiment correlates with the DSC response of the bulk material. Furthermore, activation energy E_A for isolated cross-links is almost a constant, so the M_c dependence of the width parameters can be expected to show a linear relationship between $1/(1 - \alpha)$ and M_c for the CC distribution or $1/(1 - n)$ and M_c for the WW, respectively (Figure 11).

The E_A* and width parameters of the distributions of the swollen sample are significantly reduced as compared

to those of the N650 sample. The swelling of networks involves complex processes and depends on many factors. The highly swollen network is believed to exhibit properties closer to those of the phantom network model. Our NMR results indicate that the mobility of the junction points will increase with swelling.

Conclusion

In many studies of molecular dynamics the data are analyzed by a distribution function which is implied to be a unique one or even claimed to be so explicitly. This detailed comparison of the CC and WW distribution function analysis showed that they are equally suitable. Any preference would be based on correlation with macroscopic mechanical or dielectric behaviors, which is one of the ultimate objectives of this kind of fundamental research. We have demonstrated this correlation elsewhere using the WW distribution function analysis of 2D-exchange NMR data.

Acknowledgment. This work was supported by the Cooperative University of Massachusetts–Industry Research Program.

References and Notes

(1) Dickinson, L. C.; Morganelli, P.; Chu, C. W.; Petrovic, Z.; MacKnight W. J.; Chien, J. C. W. *Macromolecules* **1988**, *21*, 338.
(2) Dickinson, L. C.; Chien, J. C. W.; MacKnight, W. J. *Macromolecules* **1988**, *21*, 2959.
(3) Dickinson, L. C.; Chien, J. C. W.; MacKnight, W. J. *Macromolecules* **1990**, *23*, 1279.
(4) Ichikawa, K.; MacKnight, W. J. *Polymer* **1992**, *33*, 4693.
(5) Shi, J. F.; Dickinson, L. C.; MacKnight, W. J.; Chien, J. C. W.; Zhang, C.; Liu, Y.; Chin, Y. H., Jones, A. A.; Inglefield, P. T. *Macromolecules* **1993**, *26*, 1008.
(6) Fox, T. G.; Loshaek, S. *J. Polym. Sci.* **1955**, *15*, 371.
(7) Abragam, A. *The Principles of Nuclear Magnetism*; Oxford University Press: London, 1961.
(8) Spiess, H. W. In *NMR, Basic Principles and Progress*; Diehl, P., Fluck, E.; Kosfeld, R., Eds.; Springer-Verlag: Berlin, Heidelberg, New York, **1978**; Vol. 15, p 55.
(9) Connor, T. M. *Trans. Faraday Soc.* **1963**, *60*, 1574.
(10) McBrierty, V. J.; Douglass, D. C. *J. Polym. Sci. Macromol. Rev.* **1981**, *16*, 295.
(11) Beckmann, P. A. *Phys. Rep.* **1988**, *171* (No. 3), 85.
(12) Garroway, A. N.; Ritchey, W. M.; Moniz, W. B. *Macromolecules* **1982**, *15*, 1051.
(13) Spiess, H. W. *Adv. Polym. Sci.* **1985**, *66*, 23.
(14) Shioya, Y.; Mashimo, S. *J. Chem. Phys.* **1987**, *5*, 87.
(15) Havriliak, S.; Negami, S. *J. Polym. Sci., Part C* **1966**, *14*, 99.
(16) Cole, K. S.; Cole, R. H. *J. Chem. Phys.* **1941**, *9*, 341.
(17) Ngai, K. L.; Rendell, R. W.; Rajagopal, A. K.; Teitler, S. *Ann. N.Y. Acad. Sci.* **1986**, *484*, 150.
(18) Ngai, K. L.; Plazek, D. J. *J. Polym. Sci. Polym. Phys. Ed.* **1986**, *24B*, 619.
(19) Ngai, K. L.; Fytas, G. *J. Polym. Sci.* **1986**, *24*, 1683.
(20) Bendler, J. T.; Shlesinger, M. F. In *Studies in Statistical Mechanics*; Shlesinger, M. F., Weiss, G. H., Eds.; North-Holland: New York, **1985**; Vol. 12, p 31.
(21) Roy, A. K.; Jones, A. A.; Inglefield, P. T. *Macromolecules* **1986**, *19*, 1356.
(22) Helfand, E. *J. Chem. Phys.* **1983**, *78*, 1931.
(23) Axelson, D. E.; Mandelkern, L. *ACS Symp. Ser.* **1979**, *10*, 181.